Research Article Vol. 33, No. 2 / 27 Jan 2025 / Optics Express 2839
Optics EXPRESS

# Realization of a high-power UV-pumped optical parametric oscillator depending on the decrease of the color center density

JIAWEI LI,[1] XUECHEN CAO,[1] YANLIN ZHANG,[1] JIE YANG,[1] PIXIAN JIN,[1,2] JING SU,[1,2] AND HUADONG LU[1,2,3,*]

[1]State Key Laboratory of Quantum Optics and Quantum Optics Devices, Institute of Opto-Electronics, Shanxi University, Taiyuan 030006, China
[2]Collaborative Innovation Center of Extreme Optics, Shanxi University, Taiyuan 030006, China
[3]National Key Laboratory of Particle Transport and Separation Technology, Tianjin, China
*luhuadong@sxu.edu.cn

**Abstract:** In this paper, a high-power UV-pumped BBO optical parametric oscillator (OPO) is presented by increasing the working temperature of the nonlinear crystal to fasten the color center recovery speed and further decrease the color center density. When the working temperature of the BBO crystal was experimentally increased from 135 °C to 185 °C, the output power was scaled up from 1.20 W to 2.17 W. The repetition rate and pulse width of the signal light were 10 kHz and 5.23 ns, respectively. By rotating the BBO crystal, the wavelength of the signal light was tuned from 409.81 nm to 581.87 nm. To the best of our knowledge, it was the highest output power for the 355 nm UV-pumped II-type critical phase-matched BBO OPO. The results are beneficial for the development of OPOs as well as in industrial and scientific research fields.

© 2025 Optica Publishing Group under the terms of the Optica Open Access Publishing Agreement

## 1. Introduction

Ultraviolet (UV)-pumped ns pulsed optical parametric oscillator (OPO) has been widely applied in industrial, medical, defense and scientific research and so on owing to its broadband coverage over the visible and near-infrared spectrum as well as the simple and robust operation. So far, three kinds of nonlinear crystals including $\beta$-BBO [1,2], LBO [3], and CLBO [4] are main candidates for generating the parametric light when the UV laser is employed as the pump source. However, compared to the LBO and CLBO crystals, the $\beta$-BBO crystal has a larger nonlinear coefficient and temperature acceptance bandwidth as well as being nearly free of deliquescence. Moreover, when the BBO crystal is cut to satisfy the type-II critical phase matching condition, it is easy to achieve an OPO with narrow bandwidth because the generated parametric lights can be directly self-filtered with the assistance of its accepted bandwidth [5]. The first UV-pumped BBO OPO was reported by Cheng et al. as early as 1988 [1]. Although they achieved the tuning characteristic of the OPO based on the homemade type-II phase matching BBO crystal, which was in good agreement with the theoretical prediction, the conversion efficiency was limited to a low level because of the low damage threshold of the used mirror. With the development of film coating and crystal preparation technologies, the performance of the UV-pumped BBO OPO was continuously and rapidly improved. Especially, in 1991, Wang et al. [6] employed a flat UV reflecting mirror outside the resonator to return the un-depleted portion of the pump laser back into the BBO crystal for pump double passing scheme and an efficient BBO OPO with the quantum conversion efficiency of 57% was achieved. Subsequently, in 2001, G. Anstett et al. [5] coated a UV-reflecting film on the output mirror of the BBO OPO resonator to reflect the pump laser for implementing the pump double passing scheme. Meanwhile, the type-II phase-matched BBO crystal was employed to replace the type-I phase-matched BBO crystal in the experiment. As a result, the bandwidth of the achieved OPO was reduced to less than 0.1 nm and the maximal

#553441 https://doi.org/10.1364/OE.553441
Journal © 2025 Received 18 Dec 2024; revised 5 Jan 2025; accepted 6 Jan 2025; published 17 Jan 2025

Optics EXPRESS

conversion efficiency of the signal light reached up to 35%. In addition, in order to further decrease the threshold of the BBO OPO, an elliptical focused pump scheme using a cylindrical lens was developed [7,8], which can effectively overcome the walk-off effect of the BBO crystal by maintaining a large beam size in the walk-off sensitive direction of the BBO crystal. However, for many fields, average power and repetition rate are becoming more important and it is difficult to find a kind of robust high repetition rate UV-pumped BBO OPO to date. In 2018, Rao et al. [9] reported a 355 nm laser-pumped BBO OPO with a repetition rate of up to 5 kHz, and the output power at 492 nm was 2.6 W. However, it was easy to find that the performance of the BBO OPO rapidly decreased when the type-I phase-matched BBO crystal was replaced by the type-II phase-matched BBO crystal for narrowing the bandwidth of the OPO because the temperature gradient caused by the strong pump absorption was approaching the temperature tolerance limits. In other words, it is very difficult to obtain a stable and efficient narrow bandwidth UV-pumped BBO OPO with a high repetition rate and average power. In order to solve these problems, in this paper, we presented a novel method to attain a high repetition rate and high average power BBO OPO with a broad tuning range, which was demonstrated by increasing the working temperature of the adopted BBO crystal to decrease the color center density. As a result, a high-performance BBO OPO with a repetition rate of 10 kHz and bandwidth of less than 1.05 nm was achieved when a 355 nm laser with a repetition rate of 10 kHz and power of 18 W was employed in the experiment. The maximal average power was 2.17 W at the wavelength of 460.27 nm. The output wavelength of the signal and idler lights can be changed from 409.81 nm to 580.87 nm and 912.95 nm to 2654.30 nm, respectively.

## 2. Experimental setup

To realize a high repetition rate OPO with high output power, an experimental setup was designed and built as shown in Fig. 1. The pump source was acted by a 355 nm UV laser which was attained by frequency-tripling of a homemade 1064 nm laser. The maximal average output power was 18 W. The repetition rate and pulse width were 10 kHz and 8.18 ns, respectively. The measured beam parameters were $M_x^2 = 3.75$ and $M_y^2 = 3.28$, respectively. To effectively decrease the threshold of the OPO by compensating for the walk-off effect of the nonlinear crystal, two cylindrical lenses $f_1$ and $f_2$ were utilized to reshape the near parallel pump light into an ellipse waist of 2.39 mm (horizontal, walk-off plane, parallel to the polarization direction) and 0.41 mm (vertical) [8]. The designed OPO consisted of $M_1$ and $M_3$, where a type-II critical phase-matched $\beta$-BBO nonlinear crystal was inserted to generate parametric light, and a pump reflector ($M_2$) was employed to implement the pump double-pass scheme, as well as to protect the output coupler $M_3$. To decrease the threshold of the OPO, the cavity length was decreased to the minimum in the experiment [10]. The distance between $M_1$ and $M_3$ was 45 mm. The input mirror $M_1$ was coated with the high transmittance (HT) film at 355 nm and high reflectivity (HR) film in the spectral region of 400-710 nm. The output coupler ($M_3$) was coated with the partial reflectivity (~70%) film at 400-700 nm and HT film at 800-900 nm. The pump reflector ($M_2$) was coated with HR film at 355 nm and HT film at 400-2600 nm. The optical films on the mirrors in the experiment were specially customized for high damage thresholds. The BBO crystal with a dimension of $12 \times 6 \times 18$ mm$^3$ was cut to $\theta = 37°$, $\phi = 30°$ for type-II critical phase matching (by Castech). The front and rear facets were coated with protective high-damage threshold anti-reflective film. The BBO crystal was placed inside a copper heat oven whose temperature was controlled by a homemade PID controller with a controlling accuracy of 0.01 °C. The BBO crystal in the heat oven was mounted on a rotational stage (PDR1C/M, Thorlabs) to control the phase-matching angle accurately for wavelength tuning. The generated signal and idler lights were separated by a dichroic mirror $M_4$ coated with HR film at 400-710 nm and HT film at 800-900 nm at 45°.

Optics EXPRESS

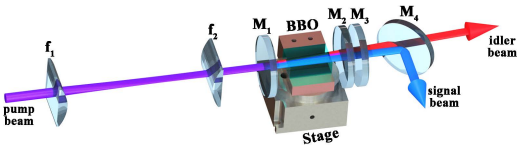



**Fig. 1.** Schematic diagram of the designed high repetition rate and high average power OPO. $f_{1,2}$: cylindrical lenses; $M_1$: input coupler; $M_2$: pump reflector; $M_3$: output coupler; $M_4$: dichroic mirror.

## 3. Results and discussion

When the BBO crystal is exposed under an intense 355 nm UV laser for the parametric light generation, the ignorable two-photon absorption (TPA) process [11,12] has to be considered because the TPA induces the formation of a mass of the color centers (absorption center, F-center) which can introduce extra spectrum features to the crystal. As a result, the generated color centers will continue to absorb the pump light as well as the parametric lights, which directly induce the very large intra-cavity loss for the designed OPO. The dynamic evolution of color center density N(t) is expressed as [13],

$$\frac{dN(t)}{dt} = \frac{\eta_f \beta_{TPA} I^2}{2\hbar\omega} - \frac{N(t)\eta_b(T)\sigma I}{\hbar\omega} \tag{1}$$

where $I$ and $\hbar\omega$ are the intensity and the photon energy of the pump laser, respectively; $\beta_{TPA} = 1.1 \times 10^{-8}$ mm/W and $\sigma = 8\times10^{-15}$ mm$^2$ [14] are the TPA coefficient and the absorption cross-section of the color center absorption, respectively; $\eta_f = 1$ and $\eta_b(T)$ are the color center formation and recovery (bleach) coefficient, respectively. The relationship between the temperature T (in Celsius) and color center recovering coefficient $\eta_b(T)$ was suggested to follow the form of Arrhenius equation [15] because a high temperature accelerates the recombination of the light-induced defect pairs in the BBO [11], which is similar to the relationship between the chemical reaction rate and temperature.

$$\eta_b(T) = A\exp(-\frac{B}{T + 273.15}) \tag{2}$$

where A and B are the unsettled numbers. By integrating Eq. (1), the time dependence of the color center density can be obtained,

$$N(t) = \frac{\eta_f \beta_{TPA} I}{2\eta_b(T)\sigma}[1 - \exp(-\frac{\eta_b(T)\sigma I}{\hbar\omega}t)] \tag{3}$$

It is obvious that $N(t)$ approaches a stabilized state with time, the stable state is,

$$N = \frac{\eta_f \beta_{TPA} I}{2\eta_b(T)\sigma} \tag{4}$$

The formed color centers can directly increase the intra-cavity loss of an OPO cavity and then limit the optical conversion efficiency and output power of the OPO. The relationship between the intra-cavity loss $l$ and the color center density $N$ for a pump-double-passed OPO cavity is [12],

$$l = 2N\sigma \cdot l_c + l_0 \tag{5}$$

where $l_c$ is the length of the BBO crystal, and $l_0$ represents the intrinsic loss caused by the cavity elements, which can be obtained by solving the relationship between the intra-cavity loss and the

Optics EXPRESS

threshold of the OPO [10]. The conversion efficiency of the OPO is [16]:

$$\eta = 0.9\frac{1-R}{1-R(1-l)}\frac{(\ln\gamma)^{2.33}}{\gamma} \tag{6}$$

where R is the reflectivity of the output coupler; $\eta = P_{\text{signal}}/P_{\text{pump}}$ is the conversion efficiency; $\gamma = P_{\text{pump}}/P_{\text{threshold}}$ is the ratio of the actual pumping power to the threshold. As a result, the power of the signal light of the designed OPO can be predicted by substituting Eq. (2), Eq. (4), Eq. (5) and Eq. (6) into:

$$P_{\text{signal}} = \eta P_{\text{pump}} \tag{7}$$

From Eq. (1)–Eq. (7), it can be seen that the working temperature of the BBO crystal directly affects the color center density $N$, which can influence the intra-cavity loss of the designed OPO and output power of the signal light.

In the experiment, when the incident pump power of the 355 nm UV laser was 18 W, the output power of the signal light for different working temperatures was first recorded and depicted in Fig. 2. When the working temperature of the BBO crystal was scanned from 135 °C to 185 °C, the output power of 460.27 nm signal light was increased from 1.20 W to 2.17 W. In this case, according to Eq. (5)–Eq. (7), the corresponding intra-cavity loss can be decreased from 0.55 to 0.13. From the variation trends of the output power and the intra-cavity loss, it can be seen that the output power and intra-cavity loss would approach the theoretical maximum value of 2.56 W and intrinsic value of 0.05, respectively, when the working temperature of the BBO crystal was scanned beyond 275 °C. According to Eq. (2) and Eq. (5), the variation trends of the color center recovery coefficient $\eta_b(T)$ and the net color center density $N$ were depicted in Fig. 3. It can be found that the color center density N decreased from $1.735 \times 10^{12}$ to $2.692 \times 10^{11}$ when the working temperature of the BBO crystal increased from 135 °C to 185 °C. At the same time, the corresponding color center recovery coefficient increased from 0.1124 to 0.7240. Based on the measured result, the relationship between the $\eta_b(T)$ and the working temperature of the BBO crystal can be expressed as $2.7 \times 10^6 \exp(-7000/(T + 273.15))$, where A and B in Eq. 2 were $2.7 \times 10^6$ and $-7000(^\circ\text{C})^{-1}$, respectively. Overall, increasing the working temperature of the BBO crystal directly increases the color center recovery coefficient $\eta_b(T)$, thereby decreasing the color center density $N$ and intra-cavity loss $l$, which is beneficial for increasing the output power of the signal light of the OPO.

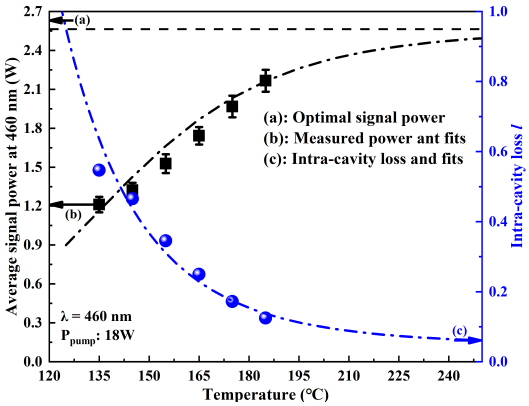



**Fig. 2.** Measured output power and corresponding intra-cavity loss versus working temperature of BBO crystal

Lastly, when the working temperature of the BBO crystal was set to 185 °C, a high-power OPO with a repetition rate of 10 kHz was achieved. The repetition rate and pulse width of the signal

Optics EXPRESS

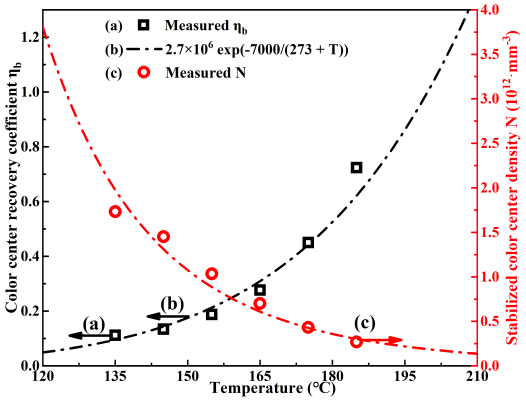



**Fig. 3.** Calculated color center recovery coefficient $\eta_b(T)$ and stabilized color center density $N$ versus working temperature of BBO crystal.

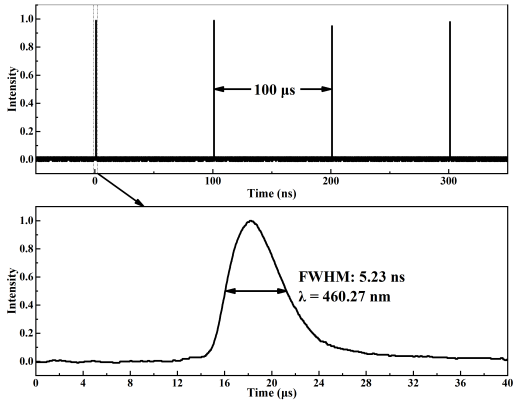



**Fig. 4.** Measured repetition rate and pulse width of signal light.

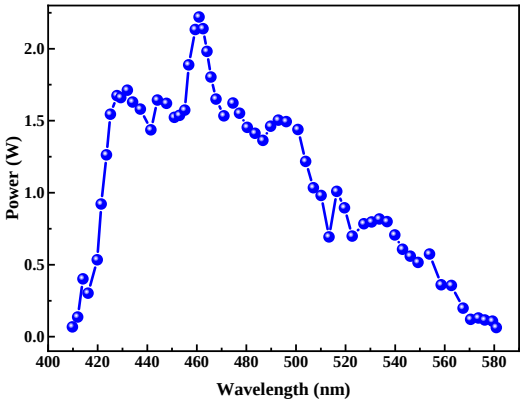



**Fig. 5.** Tuning characteristic of signal light.

Optics EXPRESS

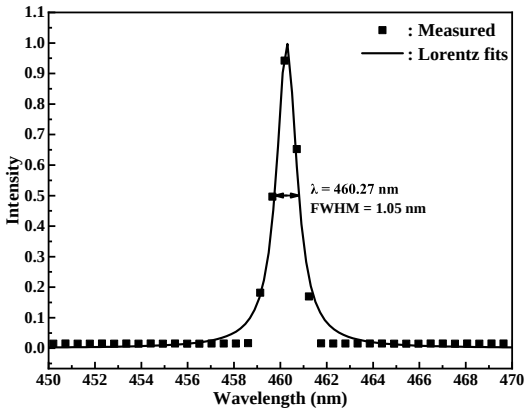



**Fig. 6.** Measured spectrum width of signal light at 460.27 nm.

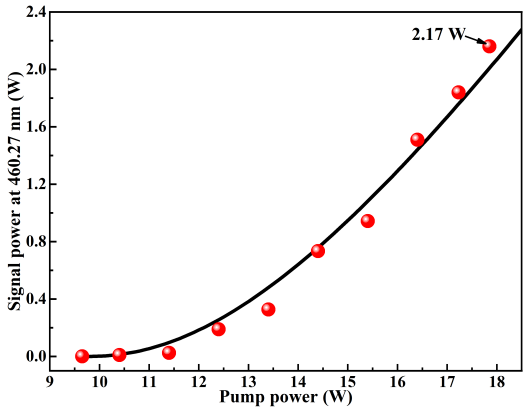



**Fig. 7.** Measured output power of signal light versus its trend.

light were 10 kHz and 5.23 ns, respectively, as shown in Fig. 4. Then the tuning characteristic of the OPO was recorded and shown in Fig. 5. It was clear that the output wavelength of the signal light can tuned from 409.81 nm to 580.87 nm, which was measured by employing a spectrometer (AMOS-UV-NIR, LBTEC). The corresponding wavelength of the idler light can change from 912.95 nm to 2654.30 nm. The maximal tuning ranges for the signal and idler lights could reach up to 171.06 nm and 1741.35 nm, respectively. When the wavelength of the OPO was tuned to near 460 nm, the spectrum width of the signal light was obtained. The measured results were fitted with the Lorentzian function, as shown in Fig. 6. The center wavelength and the spectrum width of the measured signal light were 460.27 nm and 1.05 nm, respectively. At this time, the output power curve at 460.27 nm was measured with the assistance of a power meter (S322C, Thorlabs) and depicted in Fig. 7, which showed that the threshold and optical conversion efficiency of the OPO were 9.65 W and 12.05%, respectively. The maximal power of the signal light reached 2.17 W when the maximal incident pump power was 18 W. To the best of our knowledge, it was the highest output power for the 355 nm UV-pumped II-type critical phase-matched BBO OPO. Furthermore, the beam quality of the signal light was also measured by manually recording the beam shape at different locations using a CCD camera beam profiler (BC106N-VIS/M, Thorlabs). Two cylindrical lenses were employed to reshape the signal light from an ellipse to a round shape because an ellipse pump laser was adopted in the experiment, as

Optics EXPRESS

shown in Fig. 8. The measured beam parameters were $M_x^2 = 1.79$ and $M_y^2 = 2.96$, respectively. And the beam shape of the signal light was shown in the inset of Fig. 8.

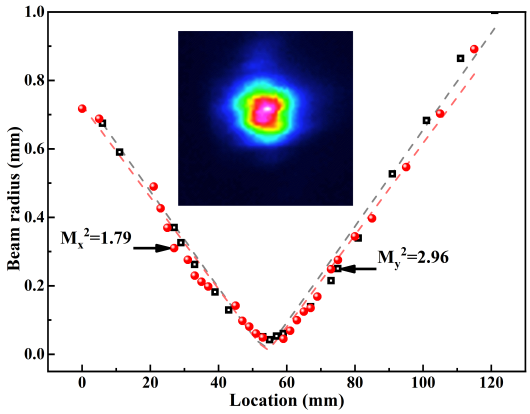



**Fig. 8.** Measured $M^2$ parameters of signal light. Inset: beam shape of signal light.

## 4. Conclusion

In conclusion, we realized a high power and narrow pulse width UV-pumped BBO OPO by increasing the working temperature of the BBO crystal to decrease the color center density. The relationship between the working temperature, color center density, intra-cavity loss, and output power of the OPO was first analyzed. Then, based on the built BBO OPO, the color center density can be obtained by measuring the output power at different working temperatures of the BBO crystal. It is clear that the output power of the UV-pumped BBO crystal can be effectively scaled up by increasing the working temperature of the BBO crystal because it was beneficial for directly decreasing the color center density and intra-cavity loss. In the experiment, when the working temperature was increased from 135 °C to 185 °C, the output power can be increased from 1.20 W to 2.17 W. The experimental results were in good agreement with the theoretical prediction. Finally, when the working temperature of the BBO crystal was set to 185 °C, a stable UV-pumped BBO OPO with an output power of 2.17 W was achieved. The repetition rate and pulse width of the signal light were 10 kHz and 5.23 ns, respectively. By rotating the BBO crystal, the wavelength of the signal light was tuned from 409.81 nm to 580.87 nm, and the maximal tuning range of the signal light was 171.06 nm. We believe that the developed method can pave the way to realize a high-power and narrow bandwidth UV-pumped BBO OPO with a high repetition rate.

**Funding.** Applied Basic Research Project of Shanxi Province, China (202103021221004); Research Project Supported by Shanxi Scholarship Council of China (2022-015); Special Fund for Science and Technology Innovation Group of Shanxi Province (202204051002005); The First Lab - National Innovation Center (Shanxi) Science and Technology Innovation Project; Funding from the National Key Laboratory of Particle Transport and Separation Technology (KWKF-2024-2).

**Disclosures.** The authors declare no conflict of interest.

**Data availability.** Data underlying the results presented in this paper are not publicly available at this time but may be obtained from the authors upon reasonable request.

## References

1. L. K. Cheng, W. R. Bosenberg, and C. L. Tang, "Broadly tunable optical parametric oscillation in $\beta - BaB_2O_4$," Appl. Phys. Lett. **53**(3), 175–177 (1988).
2. M. Wang, J. Ma, T. Lu, *et al.*, "Development of single-resonant optical parametric oscillator with tunable output from 410 nm to 630 nm," Chin. Opt. Lett. **20**(2), 021403 (2022).

Optics EXPRESS


3. H. Li, H. Zhang, Z. Bao, *et al.*, "High-power nanosecond optical parametric oscillator based on a long $LiB_3O_5$ crystal," Opt. Commun. **232**(1-6), 411–415 (2004).
4. B. Köhler, A. Nebel, and R. Wallenstein, "266 nm pumped cw mode-locked $CsLiB_6O_{10}$ (CLBO)-opo tunable in the blue and red spectral range," in *Conference on Lasers and Electro-Optics*, (Optica Publishing Group, 1999), p. CMG1.
5. G. Anstett, G. Göritz, D. Kabs, *et al.*, "Reduction of the spectral width and beam divergence of a bbo-opo by using collinear type-ii phase matching and back reflection of the pump beam," Appl. Phys. B **72**(5), 583–589 (2001).
6. Y. Wang, Z. Xu, D. Deng, *et al.*, "Highly efficient visible and infrared $\beta - BaB_2O_4$ optical parametric oscillator with pump reflection," Appl. Phys. Lett. **58**(14), 1461–1463 (1991).
7. S. Wu, G. A. Blake, S. Sun, *et al.*, "Low-threshold BBO OPO with cylindrical focusing," in *Nonlinear Optical Engineering , pp. 52–55.*, vol. 3263 M. S. Mangir, ed., International Society for Optics and Photonics (SPIE, 1998), pp. 52–55.
8. R. Bapna, C. Rao, and K. Dasgupta, "Low-threshold operation of a 355-nm pumped nanosecond $\beta - BaB_2O_4$ optical parametric oscillator," Opt. Laser Technol. **40**(6), 832–837 (2008).
9. C. S. Rao, S. Kundu, and A. K. Ray, "High repetition rate nanosecond optical parametric oscillator pumped by the third harmonic of a dpssl," Appl. Phys. B **124**(8), 163 (2018).
10. S. Brosnan and R. Byer, "Optical parametric oscillator threshold and linewidth studies," IEEE J. Quantum Electron. **15**(6), 415–431 (1979).
11. K. Takachiho, M. Yoshimura, Y. Takahashi, *et al.*, "Ultraviolet laser-induced degradation of $CsLiB_6O_{10}$ and $\beta - BaB_2O_4$," Opt. Mater. Express **4**(3), 559–567 (2014).
12. S. Gao, Y.-Z. Duan, Z.-N. Tian, *et al.*, "Laser-induced color centers in crystals," Opt. Laser Technol. **146**, 107527 (2022).
13. C. D. Marshall, S. A. Payne, M. A. Henesian, *et al.*, "Ultraviolet-induced transient absorption in potassium dihydrogen phosphate and its influence on frequency conversion," J. Opt. Soc. Am. B **11**(5), 774–785 (1994).
14. S. C. Kumar, J. C. Casals, J. Wei, *et al.*, "High-power, high-repetition-rate performance characteristics of $\beta - BaB_2O_4$ for single-pass picosecond ultraviolet generation at 266 nm," Opt. Express **23**(21), 28091 (2015).
15. K. J. Laidler, "The development of the arrhenius equation," J. Chem. Educ. **61**(6), 494–498 (1984).
16. E. Granot, S. Pearl, and M. M. Tilleman, "Analytical solution for a lossy singly resonant optical parametric oscillator," J. Opt. Soc. Am. B **17**(3), 381–386 (2000).


218.26.55.224 {ts '2025-01-17 21:35:42'}